lication. Conversations with Dr. T. Udagawa have been very helpful. This work was supported in part by the U. S. Department of Energy.

[1]J. A. Cizewski, R. F. Casten, G. J. Smith, M. L. Stelts, W. R. Crane, H. G. Börner, and W. F. Davidson, Phys. Rev. Lett. 40, 167 (1978).
[2]R. F. Casten and J. A. Cizewski, Nucl. Phys. A309, 477 (1978).
[3]J. A. Cizewski, R. F. Casten, G. J. Smith, M. R. Macphall, M. L. Stelts, W. R. Kane, H. G. Börner, and W. F. Davidson, Nucl. Phys. A323, 349 (1979).
[4]A. Arima and F. Iachello, Ann. Phys. (N.Y.) 99, 253 (1976), and 111, 201 (1978), and Phys. Rev. Lett. 40, 385 (1978).
[5]T. Kishimoto and T. Tamura, Nucl. Phys. A192, 264 (1972).
[6]T. Kishimoto and T. Tamura, Nucl. Phys. A270, 317 (1976).
[7]T. Tamura, K. Weeks, and T. Kishimoto, Phys. Rev. C 20, 307 (1979).
[8]K. Weeks and T. Tamura, to be published.
[9]A. Bohr and B. R. Mottelson, *Nuclear Structure* (Benjamin, New York, 1969), p. 239 ff.
[10]W. T. Milner, F. K. McGowan, J. O'Brian, I. Y. Lee, and J. E. Holden, Phys. Rev. C 10, 2265 (1974).
[11]H. H. Bolotin, I. Katayama, H. Sakai, Y. Fujita, M. Fujiwara, K. Hosono, T. Itahashi, T. Saito, S. H. Sie, D. Conley, D. L. Kennedy, and A. E. Stuchbery, to be published; H. H. Bolotin, private communication.
[12]R. F. Casten, J. S. Greenberg, S. H. Sie, G. A. Burginyon, and D. A. Bromley, Phys. Rev. 187, 1532 (1969).
[13]M. Hoehn and R. K. Sheline, private communication.
[14]J. E. Glenn, R. J. Pryor, and J. X. Saladin, Phys. Rev. 188, 1905 (1969).
[15]R. F. Casten, J. A. Cizewski, and C. Baktash, private communication.
[16]S. W. Yates, J. C. Cunnane, P. J. Daly, R. Thompson, and R. K. Sheline, Nucl. Phys. A222, 276 (1974).
[17]U. Götz, H. C. Pauli, K. Alder, and K. Junker, Nucl. Phys. A192, 1 (1972).
[18]K. Kumar and M. Baranger, Nucl. Phys. A122, 273 (1968).
[19]L. Wilets and M. Jean, Phys. Rev. 102, 788 (1956).
[20]In ^{196}Pt, the BET (EXP) branchings of the 2_5^+ state to the 3_1^+, 4_1^+, 2_2^+, 2_1^+, and 0_1^+ states, relative to the 0_3^+ state, were, 0.003 (0.004), 0.34 (0.02), 0.14 (0.005), 0.016 (0.003), and 0.015 (0.0001), respectively, while the branchings of the 2_6^+ state to the 2_2^+ and 2_1^+ states, relative to the 2_5^+ state, were, 0.005 (0.002) and 0.0095 (0.01), respectively. The BET (EXP) energies may be summarized: 1.38 (1.40), 1.93 (1.60), and 2.39 (1.85) MeV for the 0_3^+, 2_5^+, and 2_6^+ states, respectively. Again we see that as our predicted energies approach 2 MeV, the neglect of pure quasiparticle pair states in our collective-mode calculations becomes more serious. Their inclusion is needed to bring down the energies and to reduce some of the already small $B(E2)$'s even further. In ^{190}Os no data are available for these states. Our calculations predict the largest branching of the type above to be $2_5^+ \rightarrow 3_1^+/0_3^+ = 0.02$, with all others at least an order of magnitude smaller.

Numerical Study of the Internal Kink Mode in Tokamaks

W. Kerner
Euratom Association, Max-Planck-Institut für Plasmaphysik, D-8046 Garching, Germany

and

R. Gruber and F. Troyon
Centre de Recherches en Physique des Plasmas, Ecole Polytechnique Fédérale de Lausanne, Lausanne, Switzerland

(Received 9 August 1979)

A numerical study of the internal kink mode is performed for a family of tokamak equilibria with circular cross section and parabolic pressure profile. If the β_p values are sufficiently small, the internal kink mode becomes stable.

Internal disruptions are a key of tokamaks, significantly affecting temperature and current profiles in the plasma center. The associated instabilities are generally interpreted as current-driven resistive kink modes. The study of the ideal magnetohydrodynamic (MHD) internal kink modes is important, however, since these modes might become dominant in high-β, high-temperature plasmas. In this Letter the internal kink mode, defined as a mode with a toroidal wave number $n = 1$ which leaves the plasma boundary unperturbed, is examined in the context of ideal

MHD theory by means of the ERATO[1] code. Because of the very small growth rates of this mode, this problem is a challenge to stability codes. But this study is also complementary to the contradictory published analytic results, obtained by expansion techniques.[2-5] Bussac *et al.*[2] claim that there is β_p (defined below) stabilization of the internal kink at low β_p. Pao[3] states that there is no such effect and Galvão, Sakanaka, and Shigueoka[4] find that there is only stabilization in some regions of parameter space. Zakharov[5] agrees with Ref. 2. Our numerical results confirm the analytic results of Bussac *et al.*

In order to avoid numerical errors in the equilibrium quantities, we use an analytic family of equilibria obtained by means of a separation *Ansatz*.[6] This family is characterized by a parabolic pressure profile $p = p_0\psi^2$ and a toroidal field $B_T = (B_0^2 + C\psi^2)^{1/2}/r$, where ψ designates the poloidal magnetic flux normalized to zero at the plasma surface, r the distance to the main axis, and p_0, B_0, and C three free parameters. The flux ψ is represented on a rectangular mesh, with the boundary condition that it be constant on its contour. The geometric parameters are chosen such that, near the magnetic axis, the flux surfaces are circular and there is no triangular term. The plasma surface is only approximately circular. It is found that in the limit of large aspect ratio the effect of this noncircularity on the internal kink mode is negligible. The remaining free parameters can be chosen to be the safety factor on axis q_0, the aspect ratio ϵ^{-1} and poloidal beta $\beta_p = 8\pi\int\int p\,dS/(\mu_0 I_T^2)$ with I_T as toroidal current.

The ERATO code uses a hybrid finite-element method which, for a tokamak configuration, leads to a pessimistic evaluation of stability. At low resolution, the most unstable mode is strongly destabilized. Increasing the resolution reduces the growth rates, but does not change the ordering of the unstable modes. This makes it possible to make the most unstable mode converge unambiguously and economically by extrapolating to zero mesh size.

The normalized eigenfrequency ω is related to the true frequency γ by an Alfvén time across the main radius R_0: $\omega = [R_0(\rho)^{1/2}/B_T(R_0)]\gamma$. The density ρ is set constant. Unstable MHD modes have purely exponential growth ($\omega^2 < 0$). For typical tokamak parameters, $|\omega| = 1$ corresponds to a growth time of the order of microseconds. Since we are only interested in internal modes the plasma boundary is kept fixed.

A mode is characterized by the displacement vector $\xi(\vec{r}, t) = \xi(\psi, \theta)\exp(in\varphi + i\gamma t)$, where φ is the toroidal angle around the main axis and θ the poloidal angle around the magnetic axis. We study the $n = 1$ modes. Figure 1 shows the eigenvalues ω^2 of the most unstable modes as a function of q_0 for a large-aspect-ratio case $\epsilon^{-1} = 8.4$, $\beta_p = 1.0$, 1.2, and for a smaller aspect ratio $\epsilon^{-1} = 3.5$, $\beta_p = 1.0$. Each point on the curves is obtained by a convergence study, using up to 48 radial and 48 aximuthal points in the upper half of the plasma cross section. A satisfactory resolution of the eigenfunctions requires a strong accumulation of surfaces around the $q = 1$ surface and the $q = 2$ surface, if the latter lies within the plasma. The radial ($s \propto \psi^{1/2}$) dependence of the normal ($XI = \xi_\varphi$) and aximuthal ($ZR = \xi_\theta$) components of the displacement along the $\theta = 0$ (mid-

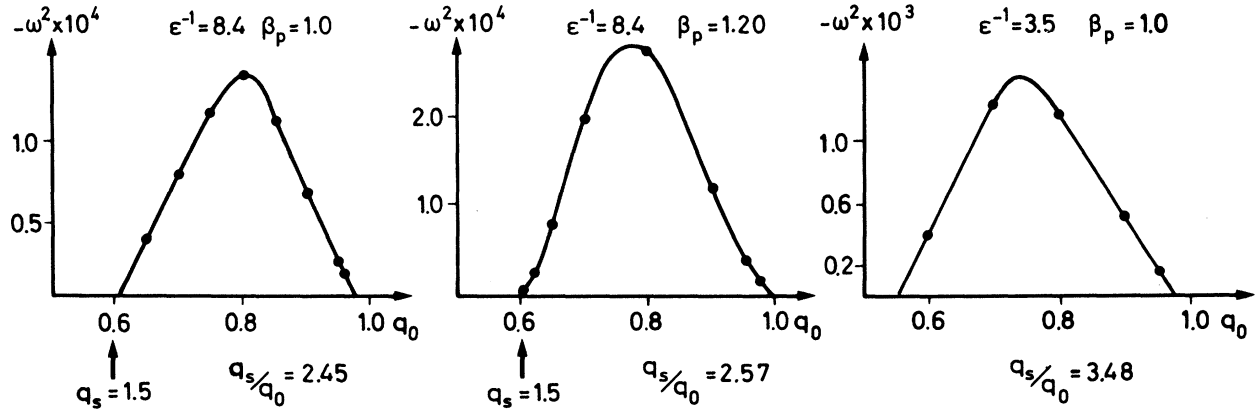

FIG. 1. The normalized eigenvalue of the most unstable mode as a function of q on axis for three different sets of parameters (q_s is q at the surface).

plane) in a particular meridian plane is shown for a typical case in Fig. 2. The corresponding vector plot of this eigenmode is shown in Fig. 3 in the same meridian plane. Moving around the main axis in the φ direction, the vortex rotates around the magnetic axis with little deformation as long as the aspect ratio is large. The characteristic step-function–like behavior of the normal component XI at the $q_0 = 1$ surface is evident in Fig. 2. At the $q = 2$ surface there is another sharp variation. There are corresponding peaks in the poloidal component ZR, which are due to the incompressible nature of the slowly growing mode. Inside the $q = 1$ surface, the mode has, in terms of Fourier components in θ, a dominant $m = 1$ contribution, whereas at the $q = 2$ surface it is essentially $m = 2$. The absolute values of the contributions to the potential energy δW on each flux surface are also shown. It is striking that the dominant negative contributions come from the region close to the axis, and that the positive ones are also inside the $q = 1.0$ surface. The negative and positive contributions cancel each other up to 3%. The very small contributions to δW between the $q = 1.0$ and $q = 2.0$ surface ($|W_i^{\pm}| \approx 10$ in the units of Fig. 2), which are not shown in the figure, are, of course, important for the correct eigenvalue.

Figure 1 shows that the unstable region is limited to a finite range of q_0 values $q_L < q_0 < q_U$. For $\epsilon^{-1} = 8.4$ and $\beta_p = 1.0$, $q_L = 0.61$ and $q_U = 0.975 < 1$. Note that at large aspect ratio $q_0 = q_L$ corresponds to $q_s = 1.5$ at the surface, which suggests that the low-q stabilization is due to interference between the $m = 1$ and $m = 2$ Fourier components of the eigenfunction. The main object of our calculations is to study the dependence of the upper stability limit q_U on β_p at large aspect ratio and compare it with the predictions of Bussac *et al.*[2]

In Ref. 2, instead of q_0 and β_p, the authors use

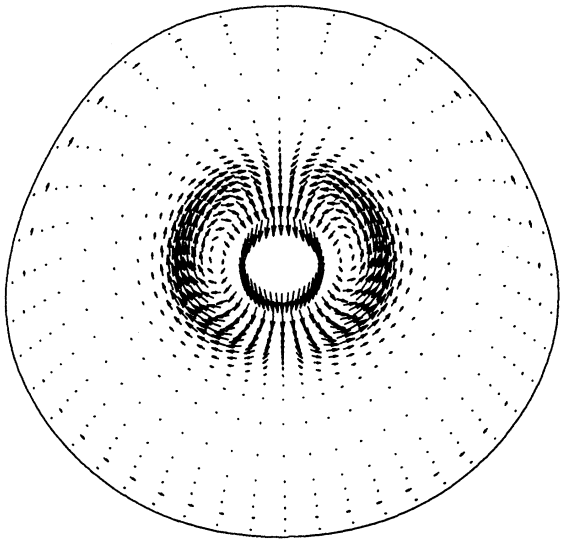

FIG. 3. Vector plot of the poloidal component of the displacement in the same meridian plane is in Fig. 2, for $\epsilon^{-1} = 8.4$, $\beta_p = 1.0$, and $q_o = 0.9$.

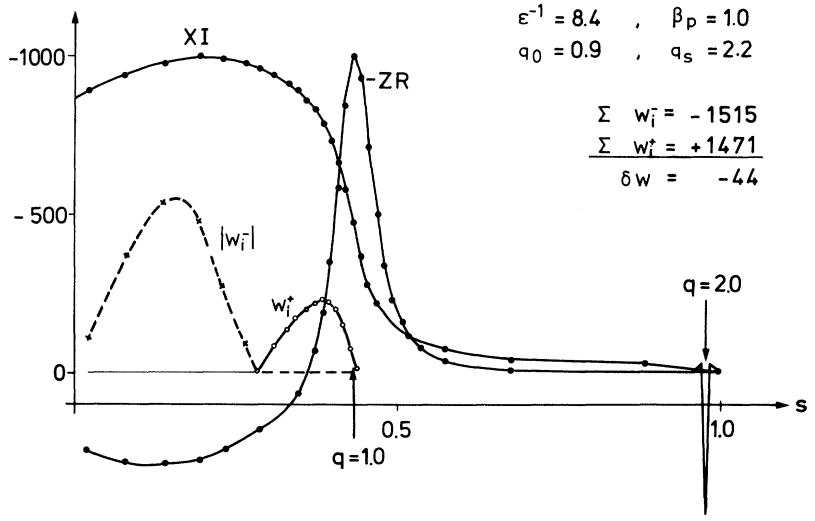

FIG. 2. Radial dependence of the normal and poloidal components XI and ZR of the displacement along the $\theta = 0$ line (midplane, outwards from the magnetic axis) in a particular meridian plane $\phi = \text{const}$. For clarity the XI has been multiplied by a constant factor of 3.5. w_i^+ and w_i^- denote positive and negative contributions of δW on each flux surface in arbitrary units ($s = 1 - \psi/\psi_{axis}$); $\delta W = \int ds\, \delta w(s) = \Sigma_i \Delta s_i\, \delta w(s_i)$.

as parameters the radius of the $q=1$ surface, r_0, and another definition of the poloidal β, denoted by us β_p^{Bussac}, which relates to ours through

$$\beta_p^{\text{Bussac}} = -\left[2\mu_0 \int_0^{r_0} \left(\frac{r}{r_0}\right)^2 \frac{dp}{dr}\, dr\right][B_p^2(r_0)]^{-1}$$

$$\approx \left[1+\frac{1}{3}\left(\frac{r_0}{a}\right)^2\right](4q_0^2)^{-1}\beta_p,$$

where B_p designates the poloidal field and a the plasma radius. The pressure profile is taken to be parabolic. The stability limit $p_{cr}^{B}(r_0)$ obtained in Ref. 2 is plotted in Fig. 4. The lines corresponding to q_0 and β_p constant are also shown. The stable region is defined as $\beta_p^{B}(r_0) \lesssim \beta_{cr}^{B}(r_0)$. The lower limit q_L has not been calculated in Ref. 2, so that there is uncertainty about the extrapolated $\beta_{cr}^{B}(r_0)$ curve, marked "?." For $\beta_p \geq 1.2$, the stability limit is always $q_0 = 1$. This same diagram shows the numerical results obtained for $\epsilon^{-1} = 8.4$. The crosses denote the values of the parameters used in the numerical stability calculations and the dots the marginal points obtained by plotting either ω^2 as a function of β_p at constant q_0, as illustrated in Fig. 5, or ω^2 as a function of q_0 at β_p, as in Fig. 1, and extrapolating to the marginal point $\omega^2 = 0$. Figure 5 shows, for $q_0 = 0.8$ and 0.9, the dependence of the eigenvalue ω^2 on β_p. It is linear in β_p. The critical values of β_p for these cases are $\beta_{cr} = 0.63$ and $\beta_{cr} = 0.70$, respectively. They agree well with Ref. 2. For $\beta_p < \beta_{cr}$ the unstable internal kink disappears. We do not see a resurgence of this mode at low β_p as predicted by Galvão, Sakanaka, and Shigueoka.[4] For $\beta_p = 1.2$, Fig. 1 confirms that $q_U = 1.0$. The numerical results are in agreement with the full stability diagram of Ref. 2.

Another important detail worth discussing is the shape of the eigenfunction at marginal stability. Inspection of the normal component XI and the poloidal component ZR of the eigenfunction for fixed $q_0 = 0.9$ and for β_p decreasing from one to β_{cr}, as done in Fig. 2, is instructive. It is found that XI as a function of s for $\theta = 0$ is straightened, with a sharper variation at the $q = 1.0$ surface, towards a true step function. At the same time the peak of ZR at the $q = 1.0$ becomes more pronounced, i.e., narrower, and the peak at the $q = 2.0$ surface vanishes. The convergence study of the eigenfunction shows that at the points of marginal stability the eigenfunction is singular at the $q = 1$ surface.

Finally, we varied the aspect ratio from 8.4 to 2.5. If the $q = 1$ surface is close to the magnetic axis, the stability limit does not change compared with the large aspect ratio cases discussed above. In Fig. 1 the eigenvalues of the unstable internal kink mode are plotted versus q_0 for an intermediate value $\epsilon^{-1} = 3.5$ and $\beta_p = 1.0$. In the range $8.4 \geq \epsilon^{-1} \geq 2.5$ and for $\beta_p = 1.0$, the upper limit remains unchanged at $q_U = 0.975$ and the lower one, q_L, decreases. The β_{cr} values for marginal stability for fixed q_0 change slightly, dropping to $\beta_{cr} = 0.5$ for $q_0 = 0.8$ and $\epsilon^{-1} = 3.5$ and $\beta_{cr} = 0.5$ for $q_0 = 0.9$ and $\epsilon^{-1} = 3.5$. It was not investigated further whether this destabilization is due to the increased

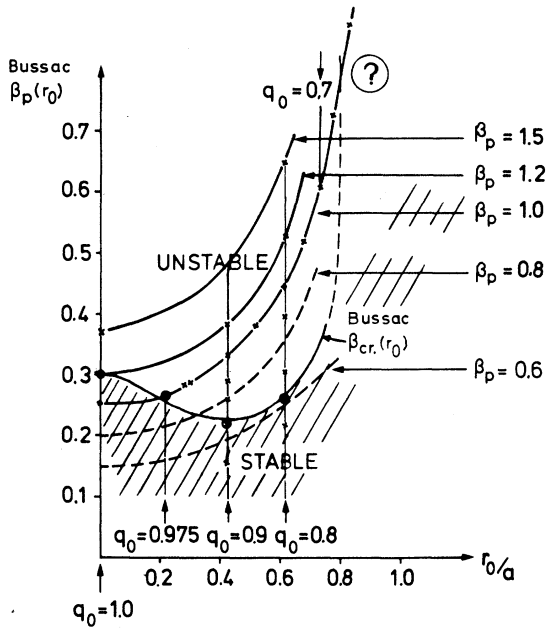

FIG. 4. Stability map for the internal kink at large aspect ratio. The curve is the theoretical curve in Ref. 2 and the dots are the numerical results for $\epsilon^{-1} = 8.4$, r_0 being the radius of the $q = 1$ surface.

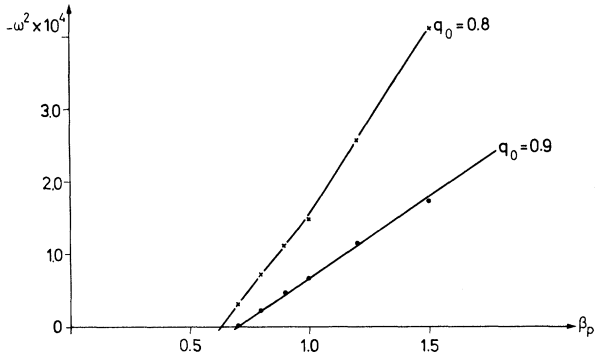

FIG. 5. The dependence of the square of the growth rate on β_p, for $\epsilon^{-1} = 8.4$ and $q_0 = 0.8$ and 0.9.

noncircularity of the outer flux surfaces or is mainly an aspect-ratio effect.

These numerical studies of the internal kink mode demonstrate the dependence of its stability on β_p in accordance with the analytic results of Bussac *et al.*,[2] but in contrast to the findings of Pao[3] and Galvão, Sakanaka, and Shigueoka.[4] For sufficiently small pressure gradients the internal kink mode becomes stable for all values of q. In the large-aspect-ratio case the results also agree quantitatively with those of Ref. 2 in stability limits and in details of the eigenfunctions, but predict up to an order-of-magnitude larger eigenvalues ω^2. The latter difference may arise from the estimate used in Ref. 2 for the kinetic energy. If the $q = 1.0$ surface is close to the magnetic axis, these stability limits remain basically unchanged up to an aspect ratio of 2.5. If, however, the $q = 1.0$ surface is farther out, as in the case of the lower stability limit $q_0 = q_L$, the results depend on the aspect ratio. These results are obtained for parabolic profiles with high shear. The fact that equilibria with a flat current have no unstable internal kink modes[1,7] indicates that the stability depends on shear, which acts as a destabilizing factor.

The authors are grateful to D. Lortz and J. Nührenberg for the use of the equilibrium solver. They also thank M. N. Bussac, R. Pellat, and J. L. Soule for interesting discussions.

[1]D. Berger, L. C. Bernard, R. Gruber, and F. Troyon, in *Proceedings of the Sixth International Conference on Plasma Physics and Controlled Fusion Research*, (International Atomic Energy Agency, Vienna, Austria, 1977), Vol. 2, p. 411.

[2]M. N. Bussac, R. Pellat, D. Edery, and J. L. Soule, Phys. Rev. Lett. 35, 1638 (1975).

[3]Y.-P. Pao, Phys. Fluids 19, 1796 (1976).

[4]R. M. O. Galvão, P. H. Sakanaka, and H. Shigueoka, Phys. Rev. Lett. 41, 870 (1978).

[5]L. E. Zakharov, Fiz. Plazmy 4 898 (1978), [Sov. J. Plasma Phys. 4, 503 (1978)].

[6]D. Lortz and J. Nührenberg, in *Proceedings of the Fifth International Conference on Plasma Physics and Controlled Fusion Research, Tokyo, Japan, 1974* (International Atomic Energy Agency, Vienna, Austria, 1975), Vol. 1, p. 439.

[7]W. Kerner, Nucl. Fusion 16, 643 (1976).

Turbulence in a Rotating Superfluid

J. T. Tough
Department of Physics, Ohio State University, Columbus, Ohio 43210
(Received 2 October 1979)

It is shown that the concepts developed for understanding superfluid turbulence in thermal counterflow can be successfully applied when the He II is also in uniform rotation. In particular, the association of a critical length scale with the turbulent transition, when extended naturally to the rotating superfluid, yields a simple result in good agreement with the data of Yarmchuck and Glaberson.

In a recent investigation of thermorotation effects in liquid helium II, Yarmchuck and Glaberson[1,2] observed several phenomena which suggest that superfluid turbulence in a rotating counterflow channel is qualitatively different from turbulence in a stationary channel. For example, the onset of the turbulence in the rotating channels occured at a larger critical heat flux. It seems paradoxical that vortex lines introduced by rotation should have this stabilizing effect on the transition to superfluid turbulence, a state which is generally believed to consist of a random distribution of vortex lines.[3,4] This Letter demonstrates that all of the observations of Yarmchuck and Glaberson are in quantitative agreement with the concepts developed to understand superfluid turbulence, in particular the relation of the critical heat flux to a critical length scale in the vortex-line distribution. This picture of a critical length scale evolved from the analysis[5] of superfluid turbulence in channels an order of magnitude smaller than those used in the rotation experiments. The extension of the critical-length criterion to these larger flow channels, and to the analysis of superfluid turbulence in rotation, constitutes a severe test of the concept.

Before considering the effects of rotation it is important to establish that the turbulence in these large channels, while stationary, is essentially the same as in the small ones. The turbulence is

